nature medicine

LETTERS

https://doi.org/10.1038/s41591-019-0561-9

Corrected: Author Correction

Liquid versus tissue biopsy for detecting acquired resistance and tumor heterogeneity in gastrointestinal cancers

Aparna R. Parikh[1,2,10], Ignaty Leshchiner[3,10], Liudmila Elagina[3,10], Lipika Goyal[1,2], Chaya Levovitz[4], Giulia Siravegna[5,6], Dimitri Livitz[3], Kahn Rhrissorrakrai[4], Elizabeth E. Martin[3], Emily E. Van Seventer[1,2], Megan Hanna[3], Kara Slowik[3], Filippo Utro[4], Christopher J. Pinto[1,2], Alicia Wong[3], Brian P. Danysh[3], Ferran Fece de la Cruz[1,2], Isobel J. Fetter[1,2], Brandon Nadres[1,2], Heather A. Shahzade[1,2], Jill N. Allen[1,2], Lawrence S. Blaszkowsky[1,2], Jeffrey W. Clark[1,2], Bruce Giantonio[1,2], Janet E. Murphy[1,2], Ryan D. Nipp[1,2], Eric Roeland[1,2], David P. Ryan[1,2], Colin D. Weekes[1,2], Eunice L. Kwak[1,2], Jason E. Faris[1,2], Jennifer Y. Wo[1,2], François Aguet[3], Ipsita Dey-Guha[1,2], Mehlika Hazar-Rethinam[1,2], Dora Dias-Santagata[1,2], David T. Ting[1,2], Andrew X. Zhu[1,2], Theodore S. Hong[1,2], Todd R. Golub[3,7,8], A. John Iafrate[1,2], Viktor A. Adalsteinsson[3], Alberto Bardelli[5,6], Laxmi Parida[4], Dejan Juric[1,2], Gad Getz[1,2,3,9*] and Ryan B. Corcoran[1,2*]

During cancer therapy, tumor heterogeneity can drive the evolution of multiple tumor subclones harboring unique resistance mechanisms in an individual patient[1–3]. Previous case reports and small case series have suggested that liquid biopsy (specifically, cell-free DNA (cfDNA)) may better capture the heterogeneity of acquired resistance[4–8]. However, the effectiveness of cfDNA versus standard single-lesion tumor biopsies has not been directly compared in larger-scale prospective cohorts of patients following progression on targeted therapy. Here, in a prospective cohort of 42 patients with molecularly defined gastrointestinal cancers and acquired resistance to targeted therapy, direct comparison of post-progression cfDNA versus tumor biopsy revealed that cfDNA more frequently identified clinically relevant resistance alterations and multiple resistance mechanisms, detecting resistance alterations not found in the matched tumor biopsy in 78% of cases. Whole-exome sequencing of serial cfDNA, tumor biopsies and rapid autopsy specimens elucidated substantial geographic and evolutionary differences across lesions. Our data suggest that acquired resistance is frequently characterized by profound tumor heterogeneity, and that the emergence of multiple resistance alterations in an individual patient may represent the 'rule' rather than the 'exception'. These findings have profound therapeutic implications and highlight the potential advantages of cfDNA over tissue biopsy in the setting of acquired resistance.

The inevitable emergence of acquired resistance is a major limitation of current targeted therapies[9]. Several key studies highlight the potential role that tumor heterogeneity plays in the emergence of resistance[3,4,7,10–14]. In acquired resistance, the evolutionary pressure of therapy can drive outgrowth of distinct tumor subclones harboring independent resistance mechanisms in an individual patient, within different metastatic lesions or within the same lesion[1,5,7,10,13]. Genomic analysis of standard single-lesion tumor biopsies on disease progression has been the mainstay of identifying mechanisms of acquired resistance, but recent studies suggest that tumor biopsies may vastly under-represent the heterogeneity of resistance in a single patient[5,7,10,15,16]. In particular, analyzing a core biopsy from one region of a single metastatic lesion may fail to detect clinically relevant resistance mechanisms, leading to mixed responses or failure of subsequent therapy[3,7,17].

Liquid biopsy—specifically, cell-free DNA (cfDNA)—may offer advantages for assessing tumor heterogeneity[4,18,19]. Tumor-derived cfDNA (also termed circulating tumor DNA) is shed from tumor cells throughout the body. Therefore, cfDNA analysis can potentially identify multiple concurrent heterogeneous resistance mechanisms in individual patients that single-lesion tumor biopsies may miss[8,20–22]. While case reports and small case series have suggested advantages of cfDNA[4,5,7,23], cfDNA and tumor biopsy have not been directly compared in larger-scale prospective patient cohorts following progression on targeted therapy.

Therefore, we evaluated a prospective cohort of molecularly defined gastrointestinal cancer patients who developed acquired resistance to targeted therapy. Through a systematic, disease center-wide liquid biopsy program, 42 patients who achieved stable disease or partial response to targeted therapy underwent liquid biopsy.

[1]Cancer Center, Massachusetts General Hospital, Boston, MA, USA. [2]Department of Medicine, Harvard Medical School, Boston, MA, USA. [3]Broad Institute of MIT and Harvard, Cambridge, MA, USA. [4]IBM Research, Yorktown Heights, NY, USA. [5]Candiolo Cancer Institute, FPO-IRCCS, Turin, Italy. [6]Department of Oncology, University of Torino, Turin, Italy. [7]Dana-Farber Cancer Institute, Boston, MA, USA. [8]Howard Hughes Medical Institute, Boston, MA, USA. [9]Department of Pathology, Massachusetts General Hospital, Boston, MA, USA. [10]These authors contributed equally: Aparna R. Parikh, Ignaty Leshchiner, Liudmila Elagina. *e-mail: gadgetz@broadinstitute.org; rbcorcoran@partners.org

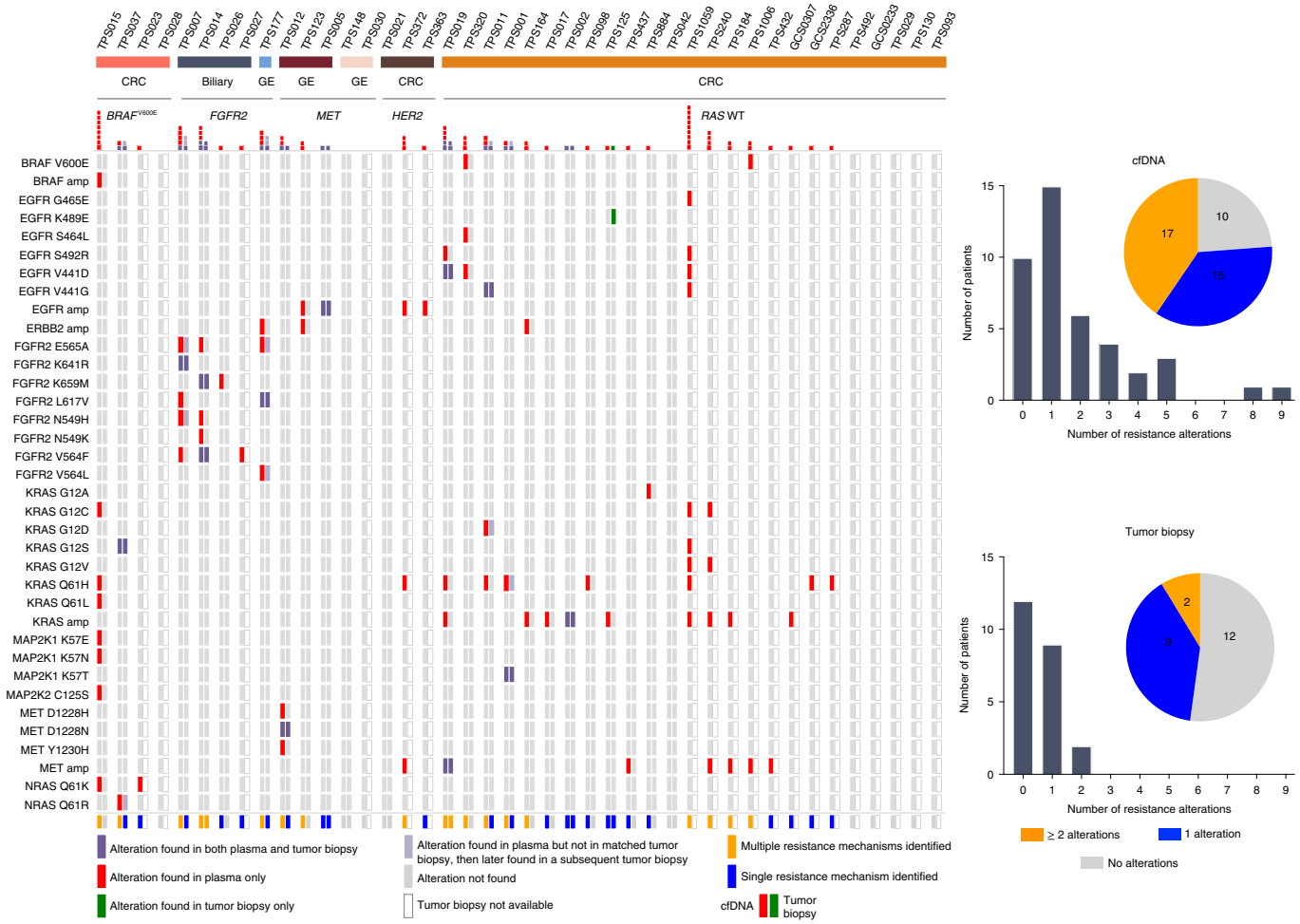

Fig. 1 | Identification of acquired resistance mechanisms in liquid versus tumor biopsy. Comparison of specific resistance alterations identified in plasma cfDNA ($n=42$) versus tumor biopsy ($n=23$) for each patient. Patients are grouped according to tumor type ($n=3$; CRC, gastroesophageal (GE) or biliary) and molecular subtype ($n=5$; *FGFR2* fusion (*FGFR2*), *MET* amplification (*MET*), *HER2* amplification (*HER2*), $BRAF^{V600E}$ or *RAS* wild type (*RAS* WT)). Red represents alterations identified in the plasma but not in the tissue biopsies. Green represents alterations identified in tissue biopsies but not in plasma. Purple represents alterations identified in both plasma and tissue biopsies. Pale purple represents alterations identified in plasma that were not detected in the postprogression tissue biopsy but were eventually detected in subsequent tissue biopsies from the same patient. The alterations detected in cfDNA versus tumor biopsy are quantified in a histogram across the top of the panel and summarized graphically to the right. The graphs on the right depict specifically the percentage of patients with one, more than one or no experimentally validated resistance alterations identified by cfDNA (top) or tumor biopsy (bottom). amp, amplification.

When possible, a matched tumor biopsy at the time of eventual disease progression was obtained (23 patients). Patients encompassed seven molecular subtypes across three tumor types (Supplementary Table 1), offering a general assessment of cfDNA on acquired resistance. To identify candidate-acquired resistance mechanisms, cfDNA isolated from postprogression plasma was analyzed by next-generation sequencing (NGS) to identify emergent alterations not detected in pretreatment tumor or cfDNA. Targeted NGS was performed in all cases, with parallel whole-exome sequencing (WES) when the tumor fraction in cfDNA was sufficient (>5%). Only previously reported and functionally validated resistance alterations were counted as resistance mechanisms[5,7,8,12,13,15,21–35] (Supplementary Table 2).

Postprogression cfDNA identified at least one previously validated resistance alteration in 32 out of 42 (76%) patients. Notably, 17 (53%) of these 32 patients (40% of all patients) exhibited >1 detectable resistance alteration (range: 2–9; median: 3 per patient), suggesting frequent and profound tumor heterogeneity associated with acquired resistance (Fig. 1 and Supplementary Table 3). In total, 78 clinically relevant resistance alterations were found in cfDNA across multiple molecularly defined tumor types receiving various targeted therapies.

To compare the effectiveness of cfDNA versus standard tumor biopsy, we analyzed matched postprogression tumor biopsies from 23 patients by WES and/or targeted NGS, and compared them with pretreatment tumor tissue. Tumor biopsy identified resistance alterations less frequently than cfDNA in only 11 out of 23 (48%) patients (Fig. 1 and Extended Data Fig. 1), whereas cfDNA identified at least one resistance alteration in 20 out of 23 (87%) patients, and in 76% of all patients. Moreover, multiple resistance alterations were identified in the postprogression biopsy in only two of the 23 cases (9%). This contrasts with cfDNA, where 40% of patients harbored multiple resistance alterations, with up to nine alterations in a single patient. Overall, postprogression cfDNA identified additional clinically relevant resistance alterations not detected in the postprogression tumor biopsies in 18 out of 23 (78%) cases.

Conversely, only one of the 23 (4%) postprogression tumor biopsies identified a resistance alteration that was not detected in matched postprogression cfDNA by NGS. In TPS125—a patient with *RAS* wild type colorectal cancer (CRC) treated with the

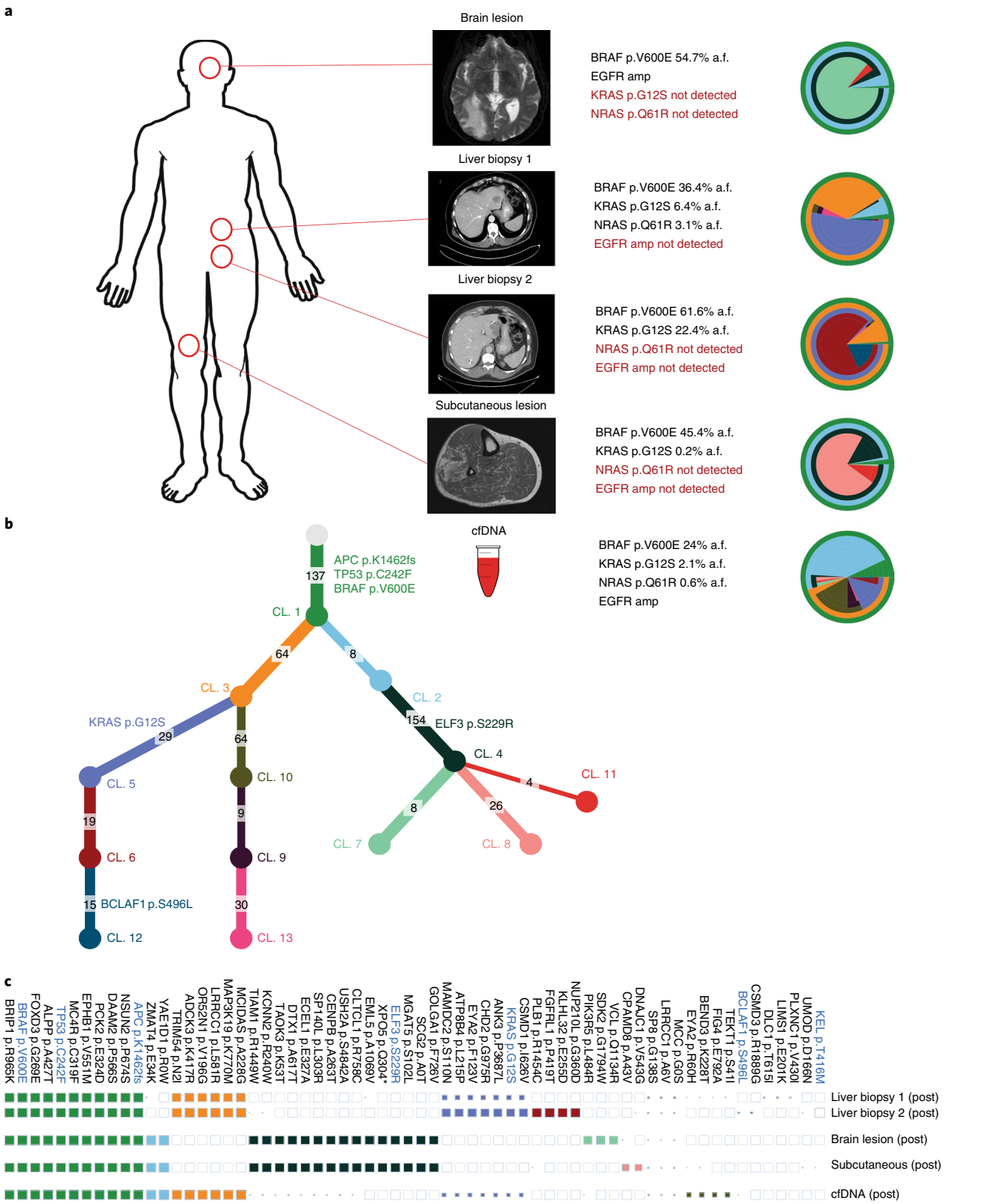

Fig. 2 | Comparison of multiple tumor biopsies versus liquid biopsy in a *BRAF*-mutant colorectal cancer patient. a, cfDNA ($n=1$) and tumor tissue biopsy specimens ($n=4$) included in the analysis for patient TPS037. For each specimen, the alterations and associated allelic fractions as determined by either ddPCR, targeted NGS or WES are shown (Supplementary Tables 3–5). All ddPCR analyses were performed to a minimum coverage depth of 300×. Layered pie charts represent the likely clonal composition of each specimen, with the color of each subclone matching the color of the respective gene and branch in the phylogenetic tree in **b**. a.f., allele frequency. **b**, Phylogenetic tree representing the clonal architecture present in the specimens (using PhylogicNDT[36]). The numbers of somatic alterations assigned to each clone (or cluster; CL) and detected events in known cancer genes appear on the branches. **c**, Representative clonal and subclonal coding of somatic alterations detected in each plasma or tissue specimen. The size of each square represents the estimated CCF of each alteration, with an empty box indicating no detection. Events in known cancer genes are highlighted in blue.

anti-epidermal growth factor receptor (EGFR) antibody cetuximab—an *EGFR*^{K489E} mutation affecting the receptor's antibody-binding domain was identified in a postprogression biopsy at 11.9% allele frequency (cancer cell fraction (CCF): 78%). *EGFR*^{K489E} was not detected by clinical NGS in postprogression cfDNA, but was detected on reanalysis using high-sensitivity droplet digital PCR (ddPCR) at 0.53% allele frequency (near the lower detection limit of clinical NGS assays for cfDNA; Supplementary Table 4). Thus, some low-level resistance alterations in rare tumor subclones may exist below the detection level in cfDNA with current technologies. Still, remarkably, every resistance alteration identified in a postprogression tumor biopsy was also detectable in matched cfDNA, suggesting that, while possible, missing resistance alterations by cfDNA analysis may be infrequent.

Interestingly, five cases with postprogression tumor biopsies had subsequent tumor specimens available for analysis, obtained during standard clinical care or through an institutional rapid autopsy program. In all cases, additional resistance mechanisms detected in postprogression cfDNA were later found in distinct metastatic lesions (Extended Data Fig. 2).

TPS037—a 53-year-old male with metastatic *BRAF*^{V600E} CRC—was treated with a combination of EGFR, BRAF and phosphoinositide 3-kinase inhibitor-α inhibitors (cetuximab, encorafenib and alpelisib; NCT01719380) for 16 months before tumor progression[15]. Biopsy of a progressing liver lesion revealed the original *BRAF*^{V600E} mutation and an emergent *KRAS*^{G12S} mutation (Fig. 2a). Postprogression cfDNA analysis by clinical NGS (Guardant360) showed not only the original *BRAF*^{V600E} and the emergent *KRAS*^{G12S} mutations, but also *NRAS*^{Q61R} and low-level *EGFR* amplification—all known resistance mechanisms in *BRAF*^{V600E} CRC[15,24,32]. Subsequently, the patient underwent: (1) resection of a brain metastasis; (2) a second protocol-related liver biopsy; and (3) biopsy of a symptomatic subcutaneous soft-tissue lesion.

To better understand the subclonal architecture of resistance, postprogression tumor specimens and cfDNA were analyzed by WES. Consistent with previous reports, the original, likely clonal, *BRAF*^{V600E} mutation persisted in all specimens (Fig. 2a). *KRAS*^{G12S} was detected by WES in both liver biopsies, but not in the brain or soft-tissue metastases. Interestingly, the brain lesion harbored an *EGFR* amplification not detected in any other tumor specimen but detected at low levels in cfDNA by clinical NGS. High-sensitivity ddPCR analysis of each tumor specimen also identified *KRAS*^{G12S} (allele frequency: 0.17%) in the subcutaneous lesion and *NRAS*^{Q61R} (allele frequency: 3.1%) in one liver biopsy (Supplementary Table 4). Thus, all three resistance alterations identified in cfDNA were identified in at least one of the postprogression tumor samples, although no single biopsy harbored all alterations. The clonal architecture and phylogenetic relationship of the four postprogression tumor biopsies and cfDNA by WES (Fig. 2b,c and Supplementary Table 5) showed shared clonal (truncal), private clonal and subclonal alterations present across various samples. Consistent with the detectability in cfDNA of all resistance alterations present in the individual tumor biopsies, each clonal alteration and the majority of subclonal mutation clusters found in different tumor biopsies were represented (at clonal or subclonal frequencies) in cfDNA, again highlighting the ability of cfDNA to capture heterogeneous molecular alterations present in distinct tumor lesions in an individual patient.

Similarly, TPS177—a 58-year-old woman with metastatic gastric adenocarcinoma harboring a fusion between *CD44* (exons 1–8) and *FGFR2* (exons 3–18)—received the FGFR inhibitor Debio1347 (NCT01948297), achieving stable disease for 4 months before progression. Serial cfDNA analysis (Fig. 3a and Supplementary Table 4) revealed an initial decrease in the abundance of a clonal founder mutation *RHOA*^{Y42C} (representative of the overall tumor burden), which rebounded rapidly on progression and was accompanied by the emergence of four *FGFR2* mutations: (1) *FGFR2*^{V564L}, affecting the gatekeeper residue in the inhibitor binding site; (2) *FGFR2*^{L617V}; and (3) *FGFR2*^{E565A} (all known mechanisms of resistance to FGFR inhibition); and (4) *FGFR2*^{S780L}, which resides outside the kinase domain and may not represent a true resistance alteration[7]. As high-level *FGFR2* fusion amplification was present (>50–150 copies), the existence of a potential passenger mutation would not be surprising. The patient underwent biopsy of a progressing para-aortic lymph node, but unfortunately expired due to disease complications. Rapid autopsy yielded 17 tumor lesions from various anatomic sites.

We analyzed WES data from pretreatment and postprogression cfDNA, postprogression biopsy and 17 autopsy specimens (Fig. 3b–d and Supplementary Table 5), and studied the clones and their phylogenetic structure with PhylogicNDT[36]. Interestingly, *FGFR2*^{V564L} (detected in postprogression cfDNA) was found predominantly in liver metastases, whereas *FGFR2*^{L617V} (also in postprogression cfDNA) had an anticorrelated pattern, predominantly detected in other metastatic sites, suggesting that these alterations confer resistance in different cell populations. *FGFR2*^{E565A}, detected in cfDNA, was identified at low levels in a single liver lesion (D). Interestingly, autopsy specimens from the stomach (M, N and O)—the primary tumor site—harbored only low levels of either resistance alteration. WES and RNA sequencing (RNA-Seq) of stomach lesions also did not detect clear evidence of the *CD44–FGFR2* fusion, and showed markedly reduced *FGFR2* expression levels and local copy numbers relative to other lesions (Fig. 3c). Phylogenetic analysis suggested that subclones present in these lesions likely represent early ancestors (Fig. 3b, upper right branch) that may have existed before development of the *CD44–FGFR2* fusion-containing clone that later seeded the majority of metastases. Thus, in these stomach lesions, resistance to FGFR inhibition may have occurred primarily due to outgrowth of an early fusion-negative clone. *FGFR2* fusion as a late event is consistent with the biology of gastric cancer, where receptor tyrosine kinase amplifications (for example, *ERBB2* or *MET*) can

Fig. 3 | Serial liquid biopsy and autopsy in a patient with *FGFR2* fusion-positive gastric cancer (TPS177). a, The allele fractions of specific alterations in cfDNA isolated from serial plasma specimens during therapy with *FGFR* inhibitor were assessed by ddPCR to a minimum coverage depth of 300×. A truncal *RHOA*^{Y42C} mutation is shown in green. Emergent candidate resistance alterations are also shown. **b**, Phylogenetic tree representing the clonal architecture across all specimens. The numbers of somatic alterations assigned to each clone (or cluster; CL) and detected events in known cancer genes appear on the branches. *FGFR2* fusion and amplification events likely occurred in the cyan subclone 2 (based on expression and copy-number patterns). *FGFR2*^{L617V} mutations were found at high levels in subclones 4 and 9. **c**, Clonal and subclonal alterations detected in each plasma ($n=2$), tumor biopsy ($n=1$) and autopsy specimen ($n=17$). The size of each square represents the estimated CCF of each alteration, with an empty box indicating no detection. *FGFR2* expression (transcripts per million (TPM)), copy number and the presence of supporting *CD44–FGFR2* fusion reads, as determined by WES and RNA-Seq, are shown, along with the number of reads for the two major *FGFR2* resistance mutations (blue, mutant; green, wild type). Boxes with diagonal lines indicate that no RNA-Seq data were available. *FGFR2* fusions were confirmed in the cfDNA samples based on off-target WES reads. **d**, Diagram of the locations of the autopsy specimens included in the analysis, along with the likely clonal migration patterns across lesions. Layered pie charts represent the estimated clonal composition of each specimen, with the color of each subclone matching the respective gene color in the branches of the phylogenetic tree. Tx, treatment.

occur as late events, leading to outgrowth of nonamplified clones during targeted therapy[30,37–39]. However, the presence of *FGFR2* resistance alterations at low levels suggests that some fusion-positive subclones may have remained in these lesions, but at levels too low to detect by WES or RNA-Seq. Overall, all three *FGFR2* mutations, and the majority of private alterations present in individual tumors, were detected in postprogression cfDNA (Fig. 3c,d).

Our data illustrate that acquired resistance to targeted therapy in gastrointestinal cancers is highly heterogeneous, often with multiple resistance alterations per patient, and that liquid biopsy can

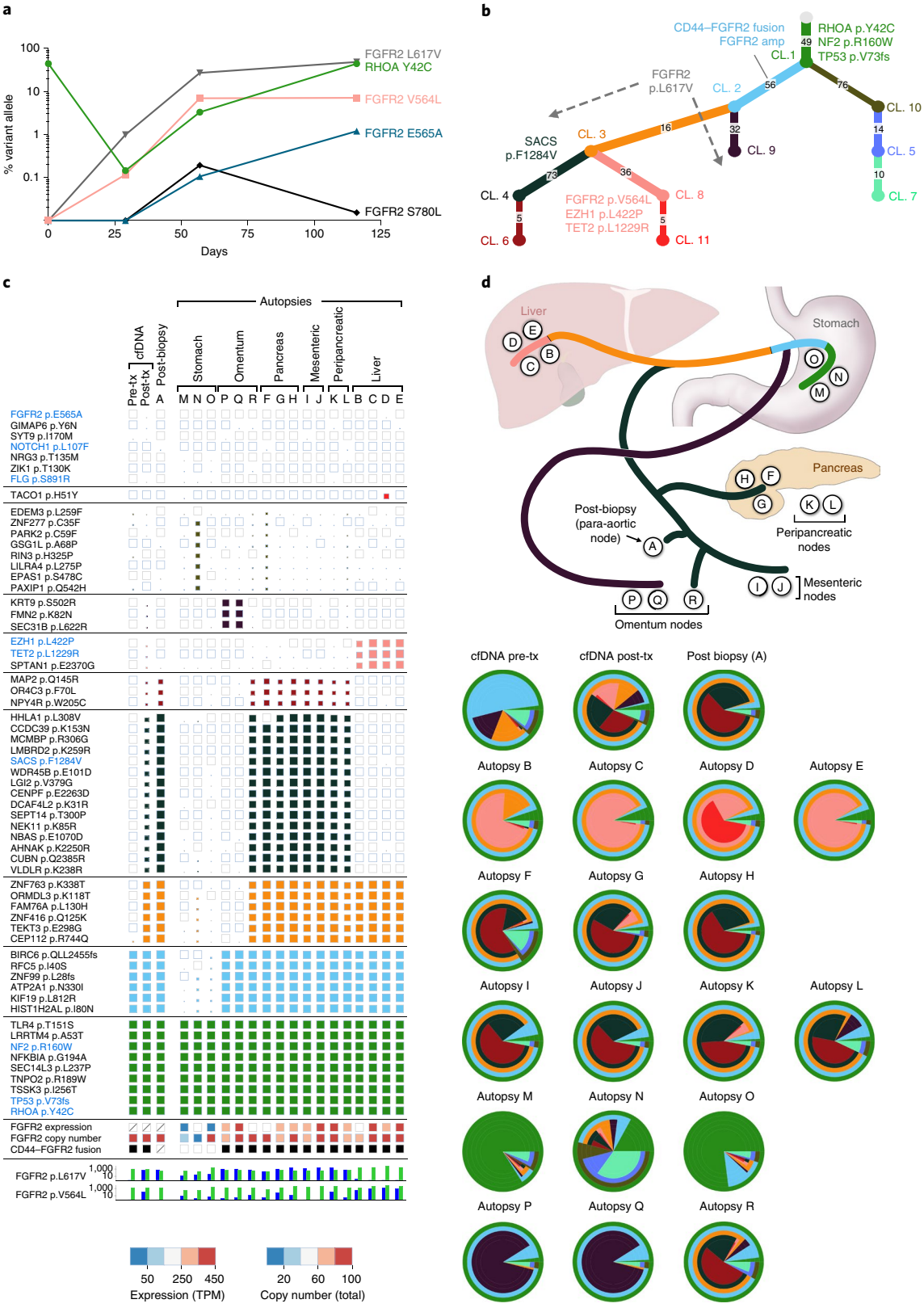

effectively detect multiple resistance alterations residing concurrently in distinct tumor subclones and different metastatic lesions. Remarkably, a resistance alteration detected in a tumor biopsy but not in the matched cfDNA by clinical NGS occurred in only one out of 23 cases. However, this alteration indeed existed in cfDNA and was detected using a higher-sensitivity method. Thus, while cfDNA analysis may miss rare tumor subclones, our study suggests effective representation of alterations from multiple lesions in cfDNA. However, cfDNA detection effectiveness may differ by tumor type or metastatic site, or in tumors with low rates of circulating tumor DNA shedding.

This study has several potential limitations. Although it represents one of the largest direct comparisons of postprogression cfDNA and matched tumor biopsy to date, overall patient numbers remain limited. Thus, additional studies may further define the degree of heterogeneity on acquired resistance and its relevance beyond gastrointestinal cancers. Additionally, in some cases, multiple biopsies and rapid autopsy confirmed that the multiple resistance alterations detected in cfDNA were derived from specific tumor lesions, but multiple tumor specimens were not available for most patients. However, in a comparator cohort of patients with similar clinical characteristics (Supplementary Table 6) with cfDNA analysis after progression on standard cytotoxic chemotherapy alone, without targeted therapy, we did not observe emergence of any of the clinically relevant resistance alterations listed in Supplementary Table 2, suggesting that resistance alterations detected in cfDNA in our study represent tumor-derived alterations emerging under selective pressure from targeted therapy. Finally, cfDNA analysis is unlikely to detect nongenetic resistance mechanisms; in 24% of cases, no resistance mechanisms were detected by cfDNA or tumor biopsy. Although analysis of alterations in these patients revealed shared patterns between copy-number alterations and tumors having a known mechanism, a clear genomic driver of resistance could not be identified (Extended Data Fig. 3 and Supplementary Table 7). Thus, tumor biopsy will still be key in assessing acquired resistance, particularly for novel or nongenetic resistance mechanisms.

In conclusion, direct comparison of cfDNA versus tumor biopsy illustrates how single-lesion tumor biopsies in the setting of acquired resistance frequently fail to identify the presence of multiple clinically relevant resistance mechanisms, with cfDNA identifying additional concurrent resistance mechanisms in 78% of cases. Thus, our data suggest that single-lesion tumor biopsy alone is inadequate for characterizing acquired resistance, and that cfDNA regularly identifies heterogeneous clinically relevant resistance alterations that are critical to the selection of subsequent therapy. This finding has important clinical implications: a treatment strategy aiming to overcome resistance will need to address the fact that a patient probably harbors multiple subclones with different resistance mechanisms. A recent study showed the effectiveness of cfDNA analysis for selecting initial molecularly directed therapy[40]. Similarly, our results support that clinical incorporation of postprogression liquid biopsy may have a valuable role in efforts to assess and overcome acquired resistance.

Online content

Any methods, additional references, Nature Research reporting summaries, source data, statements of code and data availability and associated accession codes are available at https://doi.org/10.1038/s41591-019-0561-9.

Received: 28 February 2019; Accepted: 25 July 2019;
Published online: 9 September 2019

References

1. Burrell, R. A. & Swanton, C. Tumour heterogeneity and the evolution of polyclonal drug resistance. *Mol. Oncol.* **8**, 1095–1111 (2014).
2. Gerlinger, M. et al. Genomic architecture and evolution of clear cell renal cell carcinomas defined by multiregion sequencing. *Nat. Genet.* **46**, 225–233 (2014).
3. McGranahan, N. & Swanton, C. Biological and therapeutic impact of intratumor heterogeneity in cancer evolution. *Cancer Cell* **27**, 15–26 (2015).
4. Bettegowda, C. et al. Detection of circulating tumor DNA in early- and late-stage human malignancies. *Sci. Transl. Med.* **6**, 224ra24 (2014).
5. Goyal, L. et al. Polyclonal secondary mutations drive acquired resistance to FGFR inhibition in patients with FGFR2 fusion-positive cholangiocarcinoma. *Cancer Discov.* **7**, 252–263 (2017).
6. Piotrowska, Z. et al. Heterogeneity underlies the emergence of EGFR T790 wild-type clones following treatment of T790M-positive cancers with a third-generation EGFR inhibitor. *Cancer Discov.* **5**, 713–722 (2015).
7. Russo, M. et al. Tumor heterogeneity and lesion-specific response to targeted therapy in colorectal cancer. *Cancer Discov.* **6**, 147–153 (2016).
8. Siravegna, G. et al. Clonal evolution and resistance to EGFR blockade in the blood of colorectal cancer patients. *Nat. Med.* **21**, 795–801 (2015).
9. Garraway, L. A. & Jänne, P. A. Circumventing cancer drug resistance in the era of personalized medicine. *Cancer Discov.* **2**, 214–226 (2012).
10. Gerlinger, M. et al. Intratumor heterogeneity and branched evolution revealed by multiregion sequencing. *N. Engl. J. Med.* **366**, 883–892 (2012).
11. Jamal-Hanjani, M. et al. Tracking the evolution of non-small-cell lung cancer. *N. Engl. J. Med.* **376**, 2109–2121 (2017).
12. Misale, S., Di Nicolantonio, F., Sartore-Bianchi, A., Siena, S. & Bardelli, A. Resistance to anti-EGFR therapy in colorectal cancer: from heterogeneity to convergent evolution. *Cancer Discov.* **4**, 1269–1280 (2014).
13. Misale, S. et al. Emergence of *KRAS* mutations and acquired resistance to anti-EGFR therapy in colorectal cancer. *Nature* **486**, 532–536 (2012).
14. Turajlic, S. et al. Deterministic evolutionary trajectories influence primary tumor growth: TRACERx Renal. *Cell* **173**, 595–610.e11 (2018).
15. Hazar-Rethinam, M. et al. Convergent therapeutic strategies to overcome the heterogeneity of acquired resistance in $BRAF^{V600E}$ colorectal cancer. *Cancer Discov.* **8**, 417–427 (2018).
16. Morelli, M. P. et al. Characterizing the patterns of clonal selection in circulating tumor DNA from patients with colorectal cancer refractory to anti-EGFR treatment. *Ann. Oncol.* **26**, 731–736 (2015).
17. Piotrowska, Z. et al. Heterogeneity and coexistence of T790M and T790 wild-type resistant subclones drive mixed response to third-generation epidermal growth factor receptor inhibitors in lung cancer. *JCO Precis. Oncol.* https://doi.org/10.1200/PO.17.00263 (2018).
18. Blakely, C. M. et al. Evolution and clinical impact of co-occurring genetic alterations in advanced-stage EGFR-mutant lung cancers. *Nat. Genet.* **49**, 1693–1704 (2017).
19. Haber, D. A. & Velculescu, V. E. Blood-based analyses of cancer: circulating tumor cells and circulating tumor DNA. *Cancer Discov.* **4**, 650–661 (2014).
20. Chabon, J. J. et al. Circulating tumour DNA profiling reveals heterogeneity of EGFR inhibitor resistance mechanisms in lung cancer patients. *Nat. Commun.* **7**, 11815 (2016).
21. Diaz, L. A. Jr. et al. The molecular evolution of acquired resistance to targeted EGFR blockade in colorectal cancers. *Nature* **486**, 537–540 (2012).
22. Strickler, J. H. et al. Genomic landscape of cell-free DNA in patients with colorectal cancer. *Cancer Discov.* **8**, 164–173 (2018).
23. Thierry, A. R. et al. Circulating DNA demonstrates convergent evolution and common resistance mechanisms during treatment of colorectal cancer. *Clin. Cancer Res.* **23**, 4578–4591 (2017).
24. Ahronian, L. G. et al. Clinical acquired resistance to RAF inhibitor combinations in BRAF-mutant colorectal cancer through MAPK pathway alterations. *Cancer Discov.* **5**, 358–367 (2015).
25. Arena, S. et al. MM-151 overcomes acquired resistance to cetuximab and panitumumab in colorectal cancers harboring EGFR extracellular domain mutations. *Sci. Transl. Med.* **8**, 324ra14 (2016).
26. Bahcall, M. et al. Acquired MET D1228V mutation and resistance to MET inhibition in lung cancer. *Cancer Discov.* **6**, 1334–1341 (2016).
27. Bertotti, A. et al. A molecularly annotated platform of patient-derived xenografts ("xenopatients") identifies HER2 as an effective therapeutic target in cetuximab-resistant colorectal cancer. *Cancer Discov.* **1**, 508–523 (2011).
28. Bertotti, A. et al. The genomic landscape of response to EGFR blockade in colorectal cancer. *Nature* **526**, 263–267 (2015).
29. Heist, R. S. et al. Acquired resistance to crizotinib in NSCLC with MET exon 14 skipping. *J. Thorac. Oncol.* **11**, 1242–1245 (2016).
30. Kwak, E. L. et al. Molecular heterogeneity and receptor coamplification drive resistance to targeted therapy in MET-amplified esophagogastric cancer. *Cancer Discov.* **5**, 1271–1281 (2015).
31. Montagut, C. et al. Identification of a mutation in the extracellular domain of the epidermal growth factor receptor conferring cetuximab resistance in colorectal cancer. *Nat. Med.* **18**, 221–223 (2012).
32. Oddo, D. et al. Molecular landscape of acquired resistance to targeted therapy combinations in BRAF-mutant colorectal cancer. *Cancer Res.* **76**, 4504–4515 (2016).
33. Siravegna, G. et al. Radiologic and genomic evolution of individual metastases during HER2 blockade in colorectal cancer. *Cancer Cell* **34**, 148–162.e7 (2018).

34. Tan, L. et al. Development of covalent inhibitors that can overcome resistance to first-generation FGFR kinase inhibitors. *Proc. Natl Acad. Sci. USA* **111**, E4869–E4877 (2014).
35. Yaeger, R. et al. Mechanisms of acquired resistance to BRAF V600E inhibition in colon cancers converge on RAF dimerization and are sensitive to its inhibition. *Cancer Res.* **77**, 6513–6523 (2017).
36. Leshchiner, I., et al. Comprehensive analysis of tumour initiation, spatial and temporal progression under multiple lines of treatment. Preprint at *bioRxiv* https://www.biorxiv.org/content/10.1101/508127v1(2018).
37. Janjigian, Y. Y. et al. Genetic predictors of response to systemic therapy in esophagogastric cancer. *Cancer Discov.* **8**, 49–58 (2018).
38. Kim, S. T. et al. Impact of genomic alterations on lapatinib treatment outcome and cell-free genomic landscape during HER2 therapy in HER2$^+$ gastric cancer patients. *Ann. Oncol.* **29**, 1037–1048 (2018).
39. Pectasides, E. et al. Genomic heterogeneity as a barrier to precision medicine in gastroesophageal adenocarcinoma. *Cancer Discov.* **8**, 37–48 (2018).
40. Rothwell, D. G. et al. Utility of ctDNA to support patient selection for early phase clinical trials: the TARGET study. *Nat. Med.* **25**, 738–743 (2019).

Acknowledgements

Grant Support: This work is partially supported by the NIH/NCI Gastrointestinal Cancer Specialized Program of Research Excellence P50 (CA127003, R01CA208437, K08CA166510 and U54CA224068), a Damon Runyon Clinical Investigator Award and a Stand Up To Cancer Colorectal Dream Team Translational Research Grant (grant number SU2C-AACR-DT22-17 to R.B.C.). Research grants are administered by the American Association of Cancer Research, the scientific partners of Stand Up To Cancer. The work is partially supported by the Broad/IBM Cancer Resistance Research Project (G.G. and L.P.) and the Susan Eid Tumor Heterogeneity Initiative (D.J.). The research leading to these results has received funding from FONDAZIONE AIRC under 5 per Mille 2018 ID. 21091 program – P. I. Bardelli Alberto. The research leading to these results has received funding from FONDAZIONE AIRC: AIRC Investigator Grant 2015 – ID. 16788; AIRC Investigator Grant 2018 – ID. 21923; AIRC–CRUK–FC AECC Accelerator Award – contract 22795. This work was also supported by the European Community's Seventh Framework Programme (grant agreement number 602901 MErCuRIC), H2020 (grant agreement number 635342-2 MoTriColor), IMI (contract number 115749 CANCER-ID), Ministero della Salute (project NET-2011-02352137) and Fondazione Piemontese per la Ricerca sul Cancro–ONLUS 5 per Mille 2014 and 2015 Ministero della Salute. G.S. was funded by a Roche per la Ricerca grant (2017) and AIRC three-year fellowship (2017).

Author contributions

A.R.P., I.L., L.G., D.J., G.G. and R.B.C. conceived of the study; A.R.P., I.L., L.E., L.G., C.L., G.S., D.L., K.R., E.E.M., E.E.V.S., F.U., F.F.d.l.C., I.J.F., B.N., H.A.S., F.A., I.D.-G., M.H.-R., D.D.-S., D.T.T., A.J.I., A.B., L.P., D.J., G.G. and R.B.C. performed data analysis and interpretation; I.L., L.E., C.L., D.L., K.R., E.E.M., F.U., L.P. and G.G. performed analysis of whole exome sequencing and subclonal reconstruction; A.R.P., I.L., L.G., G.S., D.D.-S., D.T.T., A.J.I., A.B., L.P., D.J., G.G. and R.B.C. supervised the data analysis; A.R.P., I.L., L.E., C.L., K.R., E.E.V.S., F.U., K.S., B.P.D., L.P., G.G. and R.B.C. participated in writing of the manuscript and generated figures; M.H., B.P.D., T.R.G., and V.A.A. suggested manuscript edits; A.R.P., L.G., E.E.V.S., C.J.P., J.N.A., L.S.B., J.W.C., B.G., J.E.M., R.D.N., E.R., D.P.R., C.D.W., E.L.K., J.E.F., D.D.-S., D.T.T., A.X.Z., J.Y.W., T.S.H., A.J.I., D.J., R.B.C., M.H., A.W., V.A. performed sample and data collection; funding was obtained by T.R.G. and G.G.; and A.R.P., I.L., E.E.V.S., C.J.P., M.H., K.S., A.W., B.P.D., and G.G. and R.B.C. participated in project administration.

Competing interests

A.R.P. is a consultant/advisory board member for PureTech, Driver, Foundation Medicine and Eisai, and has institutional research funding from Array, Plexxikon, Guardant, BMS, MacroGenics, Genentech, Novartis, OncoMed and Tolero. L.G. is a consultant/advisory board member for Debiopharm, H3 Biomedicine and Pieris Pharmaceuticals, and a steering committee member for Agios Pharmaceuticals, Taiho Pharmaceuticals and Debiopharm. E.R. is an advisory board member/consultant for Helsinn, Heron, BASF, American Imaging Management, Napo, Immuneering and Vector Oncology. D.P.R. serves on advisory boards for MPM Capital, Gritstone Oncology, Oncorus and TCR2, has equity in MPM Capital and Acworth Pharmaceuticals, and serves as an author for Johns Hopkins University Press, UpToDate and McGraw Hill. C.D.W. is a consultant for Celgene. J.E.F. is an employee at Novartis, has served as an advisory board member/consultant for Merrimack and N-of-One, and received research funding from Novartis, Roche/Genentech, Agios, Takeda, Sanofi, Celgene and Exelixis, as well as travel support from Roche/Genentech. E.L.K. is an employee of Novartis. M.H.-R. is an employee of Forma Therapeutics. D.T.T. is a consultant/advisory board member for Merrimack, Roche Ventana and EMD Millipore–Sigma, is a founder and has equity in PanTher Therapeutics, and receives research funding from ACD-Biotechne. A.X.Z. is a consultant/advisor for AstraZeneca, Bayer, Bristol-Myers Squibb, Eisai, Eli Lilly, Exelixis, Merck, Novartis and Roche/Genentech, and received research funding from Bayer, Bristol-Myers Squibb, Eli Lilly, Merck and Novartis. T.S.H. is a consultant/advisory board member for Merck and EMD Serono, and received research support from Taiho, AstraZeneca, Bristol-Myers Squibb, Mobetron and Ipsen. A.J.I. is a consultant for DebioPharm, Chugai and Roche, received research support from Sanofi and has equity in ArcherDX. T.R.G. is or has been a consultant/advisor for Foundation Medicine, GlaxoSmithKline, Sherlock Biosciences and Forma Therapeutics, and holds equity in Sherlock Biosciences and Forma Therapeutics. R.B.C. is a consultant/advisory board member for Amgen, Array Biopharma, Astex Pharmaceuticals, Avidity Biosciences, BMS, C4 Therapeutics, Chugai, Elicio, Fog Pharma, Fount Therapeutics, Genentech, LOXO, Merrimack, N-of-One, Novartis, nRichDX, Revolution Medicines, Roche, Roivant, Shionogi, Shire, Spectrum Pharmaceuticals, Symphogen, Taiho and Warp Drive Bio, holds equity in Avidity Biosciences, C4 Therapeutics, Fount Therapeutics, nRichDX and Revolution Medicines, and has received research funding from Asana, AstraZeneca and Sanofi. D.J. is an advisor/consultant for Novartis, Genentech, Eisai, Ipsen and EMD Serono, and receives research support from Novartis, Genentech, Eisai, EMD Serono, Takeda, Celgene and Placon. G.G. receives research funds from IBM and Pharmacyclics, and is an inventor on patent applications related to MuTect, ABSOLUTE, and POLYSOLVER. K.R., F.U., C.L. and L.P. are listed as co-inventors on a patent application currently pending review at the USPTO. I.L. L.E., D.L., E.E.V.S., E.E.M., M.H., K.S., C.J.P., A.W., B.P.D., F.F.d.l.C., I.J.F., B.N., H.A.S., J.N.A., L.S.B., J.W.C., B.G., J.E.M., R.D.N., F.A., I.D.-G., D.D.-S. and V.A.A. declare no competing interests.

Additional information

Extended data is available for this paper at https://doi.org/10.1038/s41591-019-0561-9.

Supplementary information is available for this paper at https://doi.org/10.1038/s41591-019-0561-9.

Reprints and permissions information is available at www.nature.com/reprints.

Correspondence and requests for materials should be addressed to G.G. or R.B.C.

Peer review information: Javier Carmona was the primary editor on this article and managed its editorial process and peer review in collaboration with the rest of the editorial team.

Publisher's note: Springer Nature remains neutral with regard to jurisdictional claims in published maps and institutional affiliations.

Methods

Patients and specimen collection. All biopsies, tumor specimens and peripheral blood draws for plasma isolation were collected in accordance with institutional review board-approved protocols. Patients provided written informed consent, and all studies were conducted in accordance with the Declaration of Helsinki. Patients provided informed written consent for blood and tissue collection as well as for genomic analysis of these specimens. Through a systematic liquid biopsy program in the Center for Gastrointestinal Cancers at the Massachusetts General Hospital Cancer Center, plasma collection for postprogression cfDNA analysis was attempted for all patients receiving targeted therapy for molecularly defined gastrointestinal cancer subtypes who achieved radiologic response or stable disease between September 2014 and March 2018. In total, 42 patients were studied. Peripheral blood was collected in two 10-ml Streck tubes on disease progression for cfDNA analysis. When possible, postprogression tumor biopsies (solid and blood) were obtained in parallel at the time of progression. These were obtained in 23 of the 42 patients. Pretreatment tumor tissue was available for analysis in all 42 cases, and pretreatment cfDNA was available in 19 cases. Rapid autopsies were performed within the first 3 h postmortem. Targeted exome sequencing on clinical tissue specimens using a Clinical Laboratory Improvement Amendments-certified clinical NGS assay was performed in the Department of Molecular Pathology at the Massachusetts General Hospital. A subset of patients for whom tumor and cfDNA specimens harbored sufficient tumor DNA content were analyzed by WES, as described below. Imaging studies, including CT and MRI scans, were obtained as part of routine clinical care. A comparator cohort of consecutive gastrointestinal cancer patients who did not receive targeted therapy, who underwent clinical NGS analysis of cfDNA (Guardant360) as part of routine clinical care after disease progression on standard cytotoxic chemotherapy (including patients who received antiangiogenic therapy, such as bevacizumab, and two patients with no previous therapy), and who had comprehensive baseline clinical tumor NGS testing and provided informed written consent as above, were also evaluated.

cfDNA isolation and analysis. Whole blood was collected by routine phlebotomy in two 10-ml Streck tubes. Plasma was separated within 1–4 d of collection through two different centrifugation steps (the first at room temperature for 10 min at 1,600*g* and the second at 3,000*g* for the same time and temperature). Plasma was stored at −80 °C until cfDNA extraction. cfDNA was extracted from plasma using the QIAamp Circulating Nucleic Acid Kit (Qiagen) according to the manufacturer's instructions.

Clinical NGS analysis of cfDNA was conducted using the Guardant360 assay. Peripheral blood was collected in two 10-ml Streck tubes and shipped for centralized processing and testing (Guardant Health) in accordance with standard clinical testing procedures. Sequencing libraries were prepared from up to 30 ng cfDNA with custom in-line barcode molecular tagging, and complete sequencing at 15,000× read depth of the critical exons in a targeted panel of 70+ genes was performed at a Clinical Laboratory Improvement Amendments-certified and College of American Pathologists-accredited laboratory (Guardant Health)[41]. Targeted NGS of cfDNA for 226 cancer-related genes using the IRCC (Instituto per la Ricerca e Cura del Cancro)-Target panel was performed as previously reported[7,8]. To identify candidate mechanisms of acquired resistance, in each case, cfDNA sequencing data from plasma obtained postprogression were compared with sequencing data from pretreatment tumor or cfDNA, as available, to identify emergent alterations not detected in the pretreatment specimens.

For the ddPCR experiments, DNA template (8–10 µl) was added to 10 µl ddPCR Supermix for Probes (Bio-Rad) and 2 µl of the custom primer/probe mixture. This reaction mix was added to a DG8 cartridge, together with 60 µl Droplet Generation Oil for Probes (Bio-Rad), and used for droplet generation. Droplets were then transferred to a 96-well plate (Eppendorf) and then thermal cycled under the following conditions: 5 min at 95 °C, 40 cycles of 94 °C for 30 s, 55 °C for 1 min and then 98 °C for 10 min (ramp rate: 2 °C s^{-1}). Droplets were analyzed with the QX200 Droplet Reader (Bio-Rad) for fluorescent measurement of fluorescein amidite and hexachloro-fluorescein probes. Gating was performed based on positive and negative controls, and mutant populations were identified. The ddPCR data were analyzed with QuantaSoft analysis software (Bio-Rad) to obtain fractional abundances of the mutant DNA alleles in the wild-type/normal background. The quantification of the target molecule was presented as the number of total copies (mutant plus wild type) per sample in each reaction. Allelic fractions were calculated as follows: allelic fraction (%) $= (N_{mut}/(N_{mut}+N_{WT}))\times 100)$, where N_{mut} is the number of mutant alleles and N_{WT} is the number of wild-type alleles per reaction. A minimum coverage depth of 300× was achieved for each analysis. ddPCR analysis of normal control plasma DNA (from cell lines) and no-DNA template controls were always included. Probe and primer sequences are available on request.

WES data. For WES, the AllPrep DNA/RNA Mini Kit (Qiagen) was used for dual extraction of both genomic DNA and RNA. DNA was quantified in triplicate using a standardized PicoGreen dsDNA Quantitation Reagent (Invitrogen) assay. The quality control identification check was performed using fingerprint genotyping of 95 common single nucleotide polymorphisms by Fluidigm Genotyping (Fluidigm). Library construction from double-stranded DNA was performed using the KAPA Library Prep Kit with palindromic forked adapters from Integrated DNA Technologies. Libraries were pooled before hybridization. Hybridization and capture were performed using the relevant components of Illumina's Rapid Capture Enrichment Kit, with a 37-Mb target. All library construction, hybridization and capture steps were automated on the Agilent Bravo liquid handling system. After postcapture enrichment, library pools were denatured using 0.1 N NaOH on the Hamilton STARlet. Cluster amplification of DNA libraries was performed according to the manufacturer's protocol (Illumina) using HiSeq 4000 exclusion amplification chemistry and HiSeq 4000 flow cells. Flow cells were sequenced utilizing sequencing-by-synthesis chemistry for HiSeq 4000 flow cells. The flow cells were then analyzed using RTA version 2.7.3 or later. Each pool of whole-exome libraries was sequenced on paired 76-cycle runs with two eight-cycle index reads across the number of lanes needed to meet coverage for all libraries in the pool.

Phylogenetic analysis of multiple samples from the same patient. WES data were analyzed on the FireCloud cloud-based analysis platform (https://portal.firecloud.org/). Somatic mutations for each tumor/normal pair were detected using the Cancer Genome Analysis WES Characterization Pipeline available on FireCloud. The WES Characterization Pipeline includes multiple steps, including MuTect[42] (for detection of somatic single nucleotide variants), Strelka[43] (for detecting small insertions and deletions), deTiN[44] (estimates potential tumor-in-normal contamination), ContEst[45] (for detecting cross-patient contamination), AllelicCapSeg[46] (for assessing allele-specific copy-number alterations) and ABSOLUTE[46] (for estimating tumor purity, ploidy, absolute allelic copy number and CCFs). The data for this study consisted of multiple samples collected from each patient (pre- and post-treatment), as well as autopsy samples. Phylogenetic analysis, subclonal reconstruction and tree building were done with the PhylogicNDT package[36].

Tumor clustering based on patterns of commonly acquired alterations. To better characterize patients with an unknown mechanism of resistance, we wanted to identify groups of patients that share similar patterns of alterations that were acquired between the pretreatment and postprogression samples. We define, for each patient with pre- and post-treatment samples, a set of features that reflect the changes in their somatic alterations between the pretreatment and postprogression samples, which we call δ (Extended Data Fig. 3a). We focused the analysis on either a list of 609 known cancer genes (Cancer Gene Census; downloaded October 2017) or a set of 5,144 genesets (MSigDB classes c2.cp and c5.bp; version 6 with at most 200 genes). We considered both point mutations (somatic single nucleotide variants, and insertions and deletions) and somatic copy-number alterations. When analyzing point mutations, we set $\delta_{gene}=1$ to reflect a significant change in CCF (that is, a change in CCF of the mutation in the gene of at least two standard deviations above the mean CCF change across all mutations, and a postprogression sample with a CCF > 0.2). Similarly, when analyzing copy number, we set $\delta_{gene}=1$ to reflect a significant copy-number change (that is, a change greater than two standard deviations above or below the mean change in copy-number levels, and amplification (copy-number level > 4) or deletion of the gene (copy-number level < 1) in the postprogression sample, respectively). To study genesets, we set $\delta_{geneset}$ to reflect the fraction of genes in the geneset that have a significant change in either copy number or mutation CCF, accounting for the size of the geneset and the total number of significant genes in the patient.

Next, to find groups of patients that have similar changes in their somatic alterations, we applied the BiMax biclustering algorithm[47] to each of the four δ matrices ($\delta^{\text{copy number}}_{\text{cancer gene}}$, $\delta^{\text{mutation}}_{\text{geneset}}$, $\delta^{\text{copy number}}_{\text{geneset}}$ and $\delta^{\text{copy number and mutation}}_{\text{geneset}}$). This analysis yielded between three and 11 biclusters (Extended Data Figs. 3b–e). To evaluate the significance of the resulting biclusters, we used a two-sided *t*-test to compare the mean size of biclusters observed in the matrix against the results from $n=10{,}000$ permuted matrices, where the values of the matrix were shuffled and biclustered.

Reporting Summary. Further information on research design is available in the Nature Research Reporting Summary linked to this article.

Data availability

Sequencing data from WES and RNA-Seq are available in the database of Genotypes and Phenotypes with the accession number phs001853.v1.p1.

References

41. Lanman, R. B. et al. Analytical and clinical validation of a digital sequencing panel for quantitative, highly accurate evaluation of cell-free circulating tumor DNA. *PLoS ONE* **10**, e0140712 (2015).
42. Cibulskis, K. et al. Sensitive detection of somatic point mutations in impure and heterogeneous cancer samples. *Nat. Biotechnol.* **31**, 213–219 (2013).
43. Kim, S. et al. Strelka2: fast and accurate calling of germline and somatic variants. *Nat. Methods* **15**, 591–594 (2018).
44. Taylor-Weiner, A. et al. DeTiN: overcoming tumor-in-normal contamination. *Nat. Methods* **15**, 531–534 (2018).
45. Cibulskis, K. et al. ContEst: estimating cross-contamination of human samples in next-generation sequencing data. *Bioinformatics* **27**, 2601–2602 (2011).
46. Carter, S. L. et al. Absolute quantification of somatic DNA alterations in human cancer. *Nat. Biotechnol.* **30**, 413–421 (2012).
47. Prelić, A. et al. A systematic comparison and evaluation of biclustering methods for gene expression data. *Bioinformatics* **22**, 1122–1129 (2006).

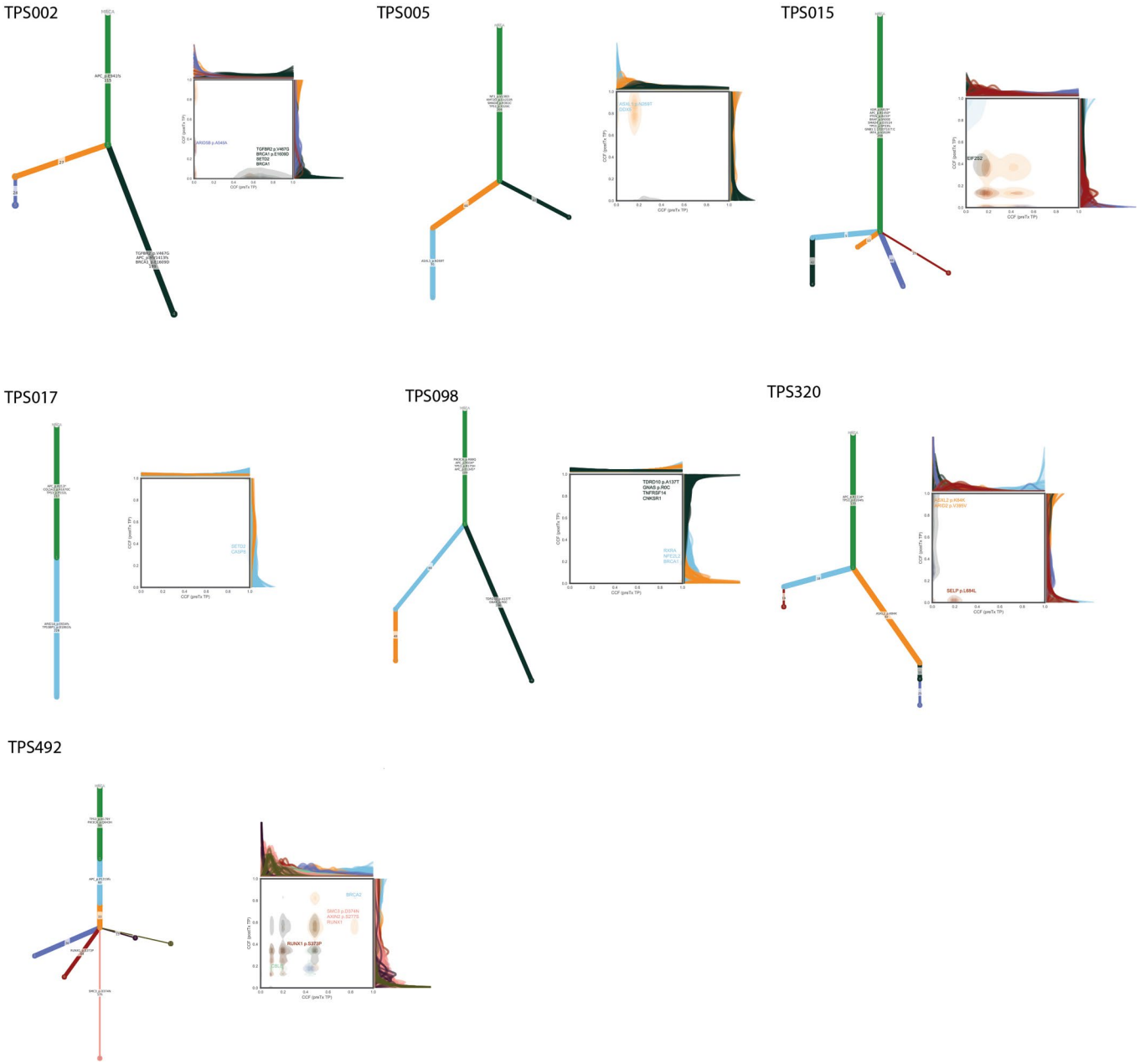

Extended Data Fig. 1 | Phylogenetic trees for paired tumor biopsies. Phylogenetic trees for patients with WES for pre- and post-treatment samples. The numbers of somatic alterations assigned to each cluster and detected events in known cancer genes appear on the branches. Two-dimensional plots show the CCF distributions of subclones in the pre- and post-treatment samples. Events in known cancers are shown next to their subclonal cluster.

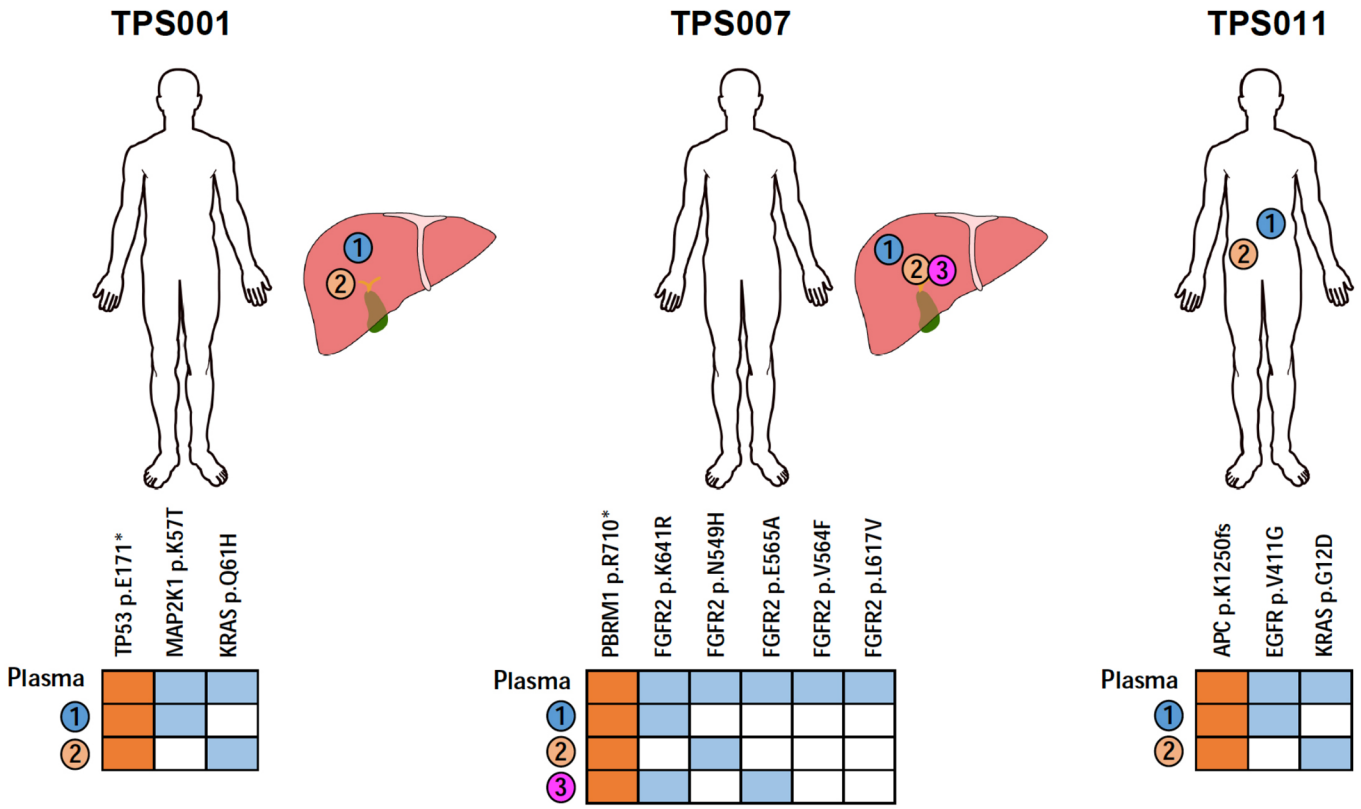

Extended Data Fig. 2 | Patients with multiple postprogression tumor biopsies. Three of five patients with multiple postprogression tumor biopsies are shown. The other two patients (TPS037 and TPS177) are shown in Figs. 2 and 3, respectively. For each patient, the location of each tumor biopsy, as well as the resistance alterations (blue) and truncal alterations (orange) detected in cfDNA and in each tumor specimen, are shown. TPS001 is a patient with *RAS* wild type colorectal cancer who developed resistance to an anti-EGFR antibody[8]. Biopsy of one liver lesion revealed an activating *MEK1* (*MAP2K1*) mutation, and biopsy of a second liver lesion identified a *KRAS* mutation. Both resistance alterations were detected in postprogression cfDNA. TPS007 is an *FGFR2* fusion-positive cholangiocarcinoma patient who developed resistance to an FGFR inhibitor[5]. Five *FGFR2* resistance mutations were identified in postprogression cfDNA, and three of these alterations were identified in distinct liver lesions harvested through a rapid autopsy program, with one lesion harboring two *FGFR2* alterations. TPS011 is a patient with *RAS* wild type colorectal cancer who developed resistance to an anti-EGFR antibody. A recurrent colon tumor harbored a *KRAS* mutation, and an *EGFR* extracellular domain mutation known to interfere with antibody binding was identified in an ovarian metastasis, whereas both alterations were detected in cfDNA. Importantly, in all patients, individual resistance mechanisms emerging in distinct metastatic lesions were detectable in cfDNA.

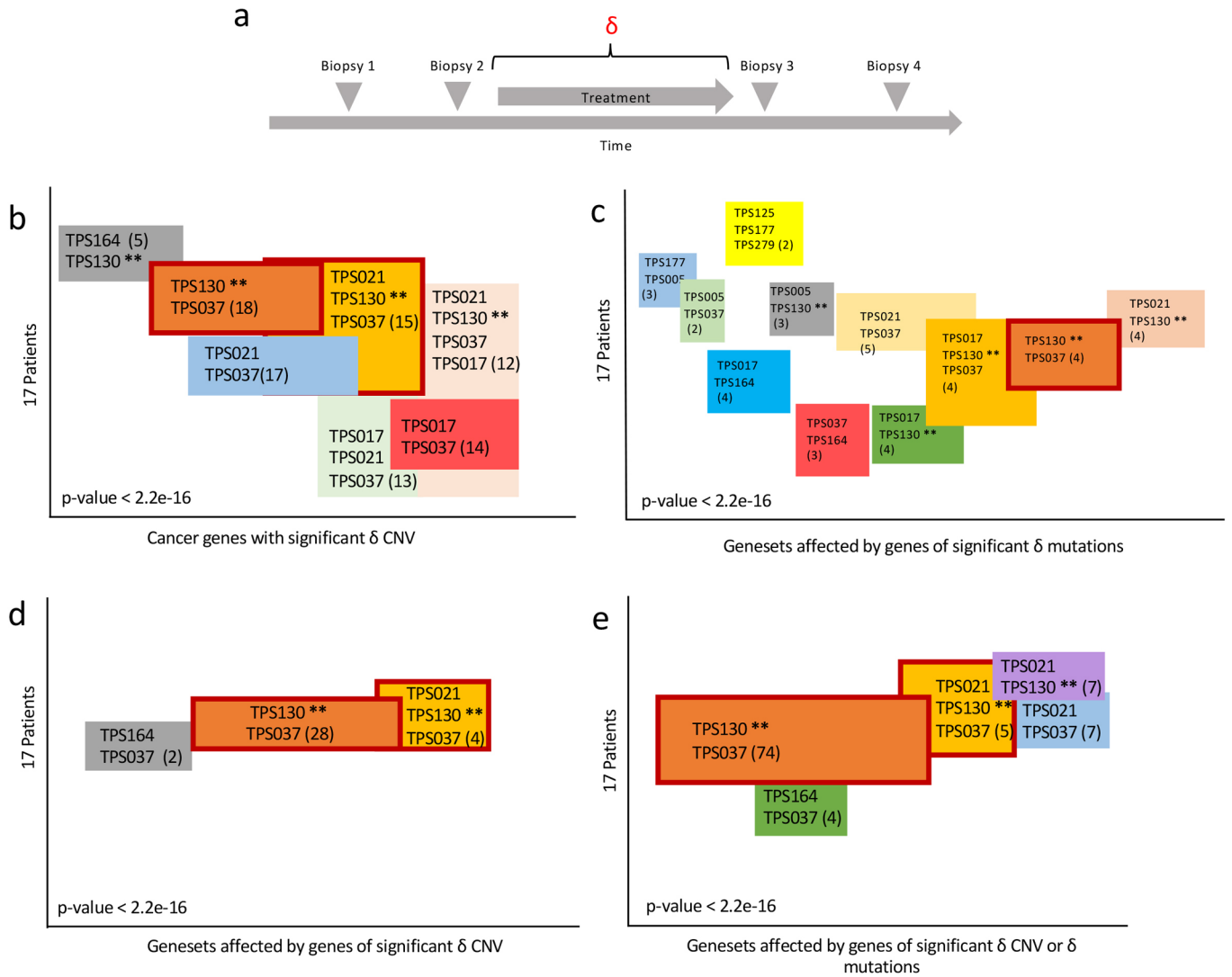

** Indicates patient with unknown MoR

Extended Data Fig. 3 | Biclusters of patients based on similar changes (δ) in somatic alteration. Biclustering of four δ matrices, reflecting changes in CCF of mutations or copy number in known cancer genes or genesets, yielded significant biclusters (all empirical *P* values < 0.0001; Methods). The biclusters from all four δ matrices included at least one bicluster with patient TPS130 (a patient with an unknown mechanism of resistance). Patient TPS130 consistently biclustered together with TPS021 and TPS037 (patients with known mechanisms of resistance) across all matrices, highlighting the possibility that additional genomic alterations contribute to resistance beyond the identified resistance alterations. **a**, The change in somatic alterations, δ, was calculated based on WES data of the samples closest to the start and end of therapy. We biclustered four δ matrices ($\delta^{\text{copy number}}_{\text{cancer gene}}$, $\delta^{\text{mutation}}_{\text{geneset}}$, $\delta^{\text{copy number}}_{\text{geneset}}$ and $\delta^{\text{copy number and mutation}}_{\text{geneset}}$) and assessed their significance by comparing the size of biclusters against $n = 10{,}000$ permuted matrices with a two-sided *t*-test (Methods). **b**–**e**, Illustration of the biclustering results (using BiMax) of the four δ matrices (biclusters are listed in Supplementary Table 6). Outlined in red are biclusters containing TPS130 observed in all four δ matrices.

nature research

Corresponding author(s): DBPR NMED-96218

Last updated by author(s): 7/23/2019

Reporting Summary

Nature Research wishes to improve the reproducibility of the work that we publish. This form provides structure for consistency and transparency in reporting. For further information on Nature Research policies, see Authors & Referees and the Editorial Policy Checklist.

Statistics

For all statistical analyses, confirm that the following items are present in the figure legend, table legend, main text, or Methods section.

n/a	Confirmed	
☐	☒	The exact sample size (*n*) for each experimental group/condition, given as a discrete number and unit of measurement
☐	☒	A statement on whether measurements were taken from distinct samples or whether the same sample was measured repeatedly
☐	☒	The statistical test(s) used AND whether they are one- or two-sided *Only common tests should be described solely by name; describe more complex techniques in the Methods section.*
☒	☐	A description of all covariates tested
☒	☐	A description of any assumptions or corrections, such as tests of normality and adjustment for multiple comparisons
☒	☐	A full description of the statistical parameters including central tendency (e.g. means) or other basic estimates (e.g. regression coefficient) AND variation (e.g. standard deviation) or associated estimates of uncertainty (e.g. confidence intervals)
☒	☐	For null hypothesis testing, the test statistic (e.g. *F*, *t*, *r*) with confidence intervals, effect sizes, degrees of freedom and *P* value noted *Give P values as exact values whenever suitable.*
☒	☐	For Bayesian analysis, information on the choice of priors and Markov chain Monte Carlo settings
☒	☐	For hierarchical and complex designs, identification of the appropriate level for tests and full reporting of outcomes
☒	☐	Estimates of effect sizes (e.g. Cohen's *d*, Pearson's *r*), indicating how they were calculated

Our web collection on statistics for biologists contains articles on many of the points above.

Software and code

Policy information about availability of computer code

Data collection	Only publicly available tools were used to collect and analyze the data, as referenced in the Methods.
Data analysis	Only publicly available tools were used to collect and analyze the data, as referenced in the Methods.

For manuscripts utilizing custom algorithms or software that are central to the research but not yet described in published literature, software must be made available to editors/reviewers. We strongly encourage code deposition in a community repository (e.g. GitHub). See the Nature Research guidelines for submitting code & software for further information.

Data

Policy information about availability of data

All manuscripts must include a data availability statement. This statement should provide the following information, where applicable:

- Accession codes, unique identifiers, or web links for publicly available datasets
- A list of figures that have associated raw data
- A description of any restrictions on data availability

Manuscript contains the following data availability statement:
Sequencing data from WES and RNA-seq will be available in dbGaP in accession number phs001853.v1.p1.
dbGaP upload is in process and data will be publicly available prior to publication.

Field-specific reporting

Please select the one below that is the best fit for your research. If you are not sure, read the appropriate sections before making your selection.

☒ Life sciences ☐ Behavioural & social sciences ☐ Ecological, evolutionary & environmental sciences

For a reference copy of the document with all sections, see nature.com/documents/nr-reporting-summary-flat.pdf

Life sciences study design

All studies must disclose on these points even when the disclosure is negative.

Sample size	Through a systematic liquid biopsy program in the Center for Gastrointestinal Cancers at the Massachusetts General Hospital Cancer Center, 42 patients receiving targeted therapy for molecularly-defined GI cancer subtypes who achieved radiologic response or stable disease were enrolled between September 2014 and March 2018.
Data exclusions	Only patients who had a response or stable disease on targeted therapy were included.
Replication	These were 42 unique patients.
Randomization	N/A
Blinding	N/A

Reporting for specific materials, systems and methods

We require information from authors about some types of materials, experimental systems and methods used in many studies. Here, indicate whether each material, system or method listed is relevant to your study. If you are not sure if a list item applies to your research, read the appropriate section before selecting a response.

Materials & experimental systems

n/a	Involved in the study
☒	☐ Antibodies
☒	☐ Eukaryotic cell lines
☒	☐ Palaeontology
☒	☐ Animals and other organisms
☐	☒ Human research participants
☐	☒ Clinical data

Methods

n/a	Involved in the study
☒	☐ ChIP-seq
☒	☐ Flow cytometry
☒	☐ MRI-based neuroimaging

Human research participants

Policy information about studies involving human research participants

Population characteristics	42 patients receiving targeted therapy for molecularly-defined GI cancer subtypes who achieved radiologic response or stable disease were enrolled between September 2014 and March 2018.
Recruitment	Patients were recruited through a systematic liquid biopsy program in the Center for Gastrointestinal Cancers at the Massachusetts General Hospital Cancer Center.
Ethics oversight	All biopsies, tumor specimens, and peripheral blood draws for plasma isolation were collected in accordance with Institutional Review Board–approved protocols, approved by the Dana-Farber/Harvard Cancer Center IRB, to which patients provided written informed consent, and all studies were conducted in accordance with the Declaration of Helsinki.

Note that full information on the approval of the study protocol must also be provided in the manuscript.

Clinical data

Policy information about clinical studies

All manuscripts should comply with the ICMJE guidelines for publication of clinical research and a completed CONSORT checklist must be included with all submissions.

Clinical trial registration	N/A
Study protocol	N/A

Data collection	N/A
Outcomes	N/A